

Ferromagnetic artificial pinning centers in superconducting Nb_{0.36}Ti_{0.64} wires

N. D. Rizzo, J. Q. Wang, and D. E. Prober^{a)}

Departments of Applied Physics and Physics, Yale University, New Haven, Connecticut 06520-8284

L. R. Motowidlo and B. A. Zeitlin^{b)}

IGC-Advanced Superconductors, Waterbury, Connecticut 06704

(Received 20 June 1996; accepted for publication 31 July 1996)

We used ferromagnetic artificial pinning centers in superconducting NbTi wires to achieve a large critical current density (J_c) in a magnetic field. Four wires were fabricated that contained nanometer-sized arrays of Ni or Fe pins inside micron-sized filaments of Nb_{0.36}Ti_{0.64} alloy. A ferromagnetic pin volume of only 2% Ni produced J_c 's (e.g., 2500 A/mm² at 5 T, 4.2 K) that were comparable to those of commercial wires that have a pin volume of ~20% Ti. We conclude that ferromagnetic artificial pins are more effective than nonmagnetic pins for a given volume percent.

© 1996 American Institute of Physics. [S0003-6951(96)02841-0]

To achieve a high critical current density (J_c) in a magnetic field, a bulk type-II superconductor must have defects or second-phase inclusions that pin the vortex lattice. The pin microstructure can be produced in NbTi—the dominant material used for commercial magnet applications—by either of two methods. The first method, used by commercial wire manufacturers, is known as the conventional approach. This consists of applying heat treatments to precipitate α -Ti out of a homogeneous Nb_{0.36}Ti_{0.64} (Nb47wt %Ti) alloy. The wire is drawn to reduce the Ti pins to nanometer thickness (~1–2 nm) and spacing (~3–6 nm).¹ The conventional approach limits the maximum Ti pin volume to approximately 21%.^{1,2} In recent years, researchers have also used a second method, artificial pinning centers (APCs), to produce pins in NbTi wires.^{3–8} Artificial pins are placed in the NbTi at a macroscopic size and then the composite wire is repeatedly drawn to produce nanometer pin thickness and spacing. The artificial pin materials used have been either Nb or Ti (low-field superconductors), or Cu (a normal metal). The optimum pin volume has been between 20% and 30%.

We report here on the properties of NbTi wires that contain ferromagnetic artificial pins. Because a ferromagnet strongly suppresses superconductivity, even a small ferromagnetic region can be a strong pin. The coherence length for superconductivity penetrating into a ferromagnet is very short ($\xi_{Ni} \sim 1$ nm),⁹ compared to that for nonmagnetic pin materials ($\xi_{Cu} > \xi_{Ti} \sim \xi_{Nb} \sim 15$ nm).¹⁰ Therefore, a small ferromagnetic pin can significantly depress the order parameter and create a large *effective* pin volume; this effect of ferromagnetic pins is observed in our wires.

We made wires that had nanometer-sized arrays of Ni or Fe pins inside micron-sized filaments of Nb_{0.36}Ti_{0.64} alloy. Ni pins in NbTi produced J_c 's (e.g., 2500 A/mm² at 5 T) that were comparable to those of commercial NbTi wire. However, the Ni pin volume was only 2%, in contrast to the optimum nonmagnetic pin volumes of 20%–30%.^{3–8} These results and those for our other wires that contained Ni pins,

indicate that wires with larger volumes of Ni may have even larger J_c 's.

Four wires were produced; each had an approximate ferromagnetic pin volume of 2%. Wires A, B, and D had a total pin volume of 3%: 2% Ni or Fe, with 1% Cu. Wire C had a total pin volume of 5%: 2% Ni with 3% Cu. Each pin consisted of the ferromagnetic core surrounded by a Cu sleeve. The sleeve was a diffusion barrier that prevented brittle intermetallics from forming between the ferromagnet and the NbTi during hot extrusion.

We developed a novel method to put the pins into the NbTi matrix for wires A, B, and D. NbTi rods were stacked in a hexagonal close-packed pattern and pin rods were put into the interstitial spaces [see Fig. 1(a)]. This interstitial approach allows the use of small pin volume percentages (1%–3%) without the need to drill holes in the NbTi rods for the pins.

For wire C, a hole was gun-drilled in a NbTi rod and the pin rod was put inside. This composite rod of NbTi and one pin was placed in a Cu can and hot extruded at 650 °C. After cold drawing to reduce its diameter further, we cut the composite rod into pieces, etched away the Cu (can) cladding, and stacked the pieces in a hexagonal pattern [see Fig. 1(b)].

A standard restack and draw process was used to reduce

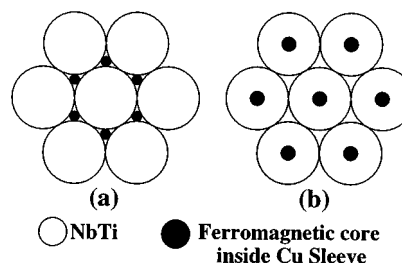


FIG. 1. Cross section of APC wire filaments before extrusion. (a) Interstitial approach: pin fills interstitial hole between NbTi rods, (b) gun-drilled approach: pin fills gun-drilled hole in center of NbTi rod. Actual filaments contain ~100 pins (wires B and D) or ~6000 pins (wires A and C) along with the appropriate number of NbTi rods.

^{a)}Electronic mail: daniel.prober@yale.edu

^{b)}Present address: APD Cryogenics, Inc., Allentown, PA 18103.

TABLE I. Description of wires made.

Wire	Pin material (vol. %)	Pin type	Filament type	Filament diameter at F_p^{\max} (μm)
A	Ni/Cu (2/1)	interstitial	large	2
B	Ni/Cu (2/1)	interstitial	small	0.2
C	Ni/Cu (2/3)	gun-drilled	large	2
D	Fe/Cu (2/1)	interstitial	small	0.2

the pins to nanometer size and spacing. The hexagonal bundle of rods was first placed into a Cu can and then extruded at a temperature of 650 °C. Cold drawing was used to reduce the diameter of the wire further. The wire was cut into 61 pieces which were then restacked in another hexagonal pattern in one of two ways: with the Cu (can) cladding left on (wires B and D) or with the cladding chemically etched off (wires A and C). Thus, wires A and C had a superconducting filament diameter (d_{fil}) that was ~ 10 times larger than that of wires B and D.¹¹ Subsequent wire processing was identical for all wires. Each hexagonal bundle was placed in a Cu tube and again cold drawn to reduce the wire diameter. Leaving the Cu (tube) cladding on, we repeated the restack and draw process two more times and ultimately reduced the multifilamentary wire to a diameter as small as 0.1 mm. A description of all the samples is given in Table I.

The critical currents (I_c) of the wires were measured using the standard 4-probe technique in transverse magnetic fields from 1 to 9 T. A resistivity criterion of $10^{-12}\Omega\text{ cm}$ was used to determine I_c . J_c was defined as I_c divided by the combined area of the NbTi and the pins (ferromagnetic core with Cu sleeve); this area was determined using a standard etch and weight technique. [For wires B and D, we did not include the area of the Cu (can) cladding between the small filaments in the calculation of J_c .] F_p is the bulk pinning force density of the wire and is defined as $F_p = J_c B$,

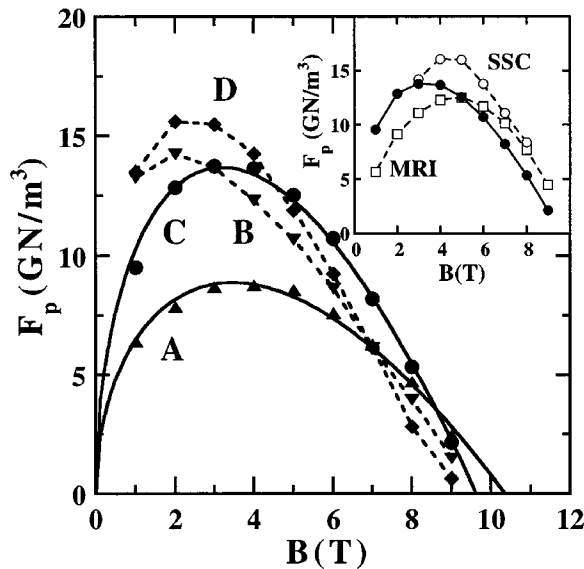


FIG. 2. Bulk pinning force $F_p = J_c B$ vs transverse applied magnetic field B : (\blacktriangle) wire A; (\blacktriangledown) wire B; (\bullet) wire C; (\blacklozenge) wire D. Dotted lines for wires B and D are guides to the eye. Solid lines for wires A and C are fits to the function $F_p \propto b^{1/2}(1-b)$. Inset: F_p vs magnetic field B for wire C (\bullet) and two conventional wires (MRI and SSC). Lines are guides to the eye.

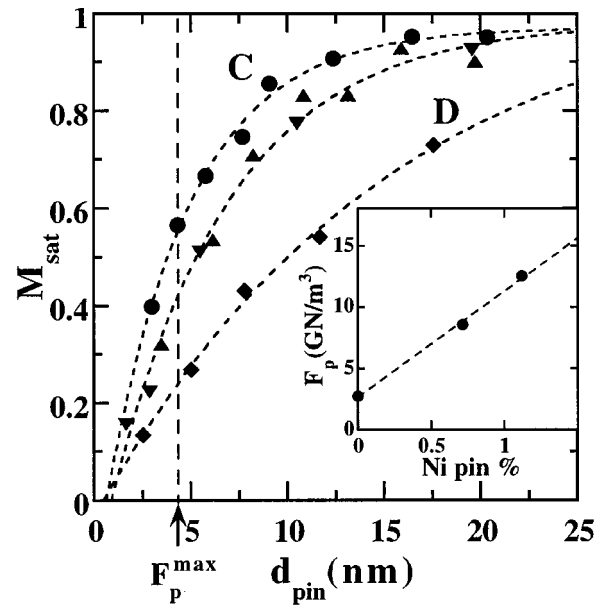


FIG. 3. Average saturation magnetization (M_{sat}) vs pin diameter (d_{pin}): (\blacktriangle) wire A; (\blacktriangledown) wire B; (\bullet) wire C; (\blacklozenge) wire D; M_{sat} for each type of pin was normalized to the value for the largest measured pin diameter (≥ 1500 nm), which was usually within 5% of the bulk value for M_{sat} . Lines are guides to the eye. Inset: F_p at 5 T vs volume percentage of Ni that remained ferromagnetic (derived from M_{sat} measurements) in wires A and C. F_p for 0% Ni is from measurements of cold-worked NbTi (see Ref. 2).

where B is the applied magnetic field. The F_p dependence on B for the wires that had maximum J_c are shown in Fig. 2. The ferromagnetic pin diameter was ~ 4.5 nm and the pin spacing (center to center) was ~ 30 nm in all the wires shown.

Although all the wires had approximately the same volume of ferromagnet (2%), wires B and D had additional pinning because of small filament size. A comparison between wires A and B showed that the reduced filament size increased F_p by $\sim 5-7$ GN/m³ for $B \sim 1-3$ T; the magnitude of this increase was comparable to that observed in other wires that had submicron NbTi filaments separated by Cu^{4,12}. We attribute the additional pinning to the interfaces between the Cu (can) cladding and the small NbTi filaments ($d_{fil} \sim 0.2 \mu\text{m}$). For Wires A and C ($d_{fil} \sim 2 \mu\text{m}$), the interfaces were far enough apart (had lower density) so that they did not contribute significantly to F_p . We conclude that the gun-drilled Ni pins produce larger F_p than the interstitial Ni or Fe pins alone. We discuss this below.

In the inset of Fig. 2, we compare the F_p for wire C with that of conventional wire used to make resonance imaging magnets (MRI) and magnets for the Superconducting Super-Collider (SSC)¹³. Both of these conventional wires contained a precipitated Ti pin volume of 17%–20%, in contrast to the 2% Ni in our wires. [The 3% Cu diffusion barrier probably made no significant direct contribution to F_p (see below).]¹⁴ Thus, we conclude that ferromagnetic pins are more effective than nonmagnetic pins for a given volume percent.

Despite their relative strength, the effectiveness of the ferromagnetic pins was probably reduced by some pin material becoming nonmagnetic at optimum size. If a pin becomes partly nonmagnetic, then it will not depress the order parameter as much as if it were fully ferromagnetic, and the

effective pin volume will be reduced. The evidence for the loss of ferromagnetic material is shown in Fig. 3. We measured the average saturation magnetization (M_{sat}) of the pins using a SQUID magnetometer at a temperature of 12 K, well above the T_c of NbTi ($T_c \sim 9$ K). The loss of magnetization for Fe was much larger than that for Ni. However, the bulk M_{sat} of Fe is three times greater than that of Ni; this may explain why F_p is comparable for wires B and D. At optimum pin size ($d_{\text{pin}} \sim 4$ nm), almost 50% more Ni remained ferromagnetic in wire C than in wires A and B. This correlates with the larger F_p of wire C compared to wire A.

Because of the nanometer pin sizes, the reasons for the loss of magnetic material were difficult to determine. We speculate that as a result of cold work, some mechanical mixing of the ferromagnet and the NbTi occurred at the nanometer size scale, thus producing a nonmagnetic (or less strongly magnetic) alloy. The Fe pins deformed under mechanical strain even at intermediate size, while the Ni pins maintained a relatively uniform shape. This would explain the more severe loss of magnetization for Fe compared to Ni. The gun-drilled Ni pins had a thicker Cu barrier and a rounder shape at intermediate size than the interstitial Ni pins; consequently, M_{sat} of wire C was higher than that of wires A and B at optimum pin spacing.

By combining the M_{sat} results with the F_p measurements, the dependence of F_p on the Ni volume percentage remaining ferromagnetic can be observed (see Fig. 3; inset); the trend shown is very promising. It is clear that a further increase of F_p may be possible with an increase in the volume of Ni in the wires. Wires with larger Ni volumes are currently being fabricated.

The maximum F_p for our wires occurred at lower fields than for conventional wires. We believe this shift to lower fields is a result of the smaller pin number densities in our wires. In optimized conventional wires, the pins are elongated Ti ribbons that are closely spaced ($\sim 3\text{--}6$ nm).¹ In contrast, our APC wires had round pins ($d_{\text{pin}} \sim 4$ nm) with a larger optimum pin spacing (~ 30 nm). Thus, the maximum F_p , where the pin and vortex densities are comparable, will occur at lower fields for the APC wires than for the conventional wires.

To approximate the dependence of F_p on B more quantitatively, we assume a direct summation of pin strengths. In direct summation, $F_p = n_p f_p$, where n_p is the effective number of pins/unit volume and f_p is the force of one pin. We define $n_p = (\text{vortices/unit area})(\text{pins/unit vortex length})$. As B increases, the vortex spacing eventually becomes less than the pin spacing; when this occurs, the average number of pins/unit vortex length will decrease as $B^{-1/2}$.¹⁵ Since the

vortices/unit area increase as B , we have $n_p \propto b^{1/2}$, where $b = B/H_{c2}$ and H_{c2} is the upper critical field of the superconductor. Assuming core pinning, we also have $f_p \propto (1-b)$, which reflects the condensation energy loss as B approaches H_{c2} . Thus we expect $F_p \propto b^{1/2}(1-b)$.¹⁶ A fit of this functional form for F_p to the data for wires A and C is shown in Fig. 2 and is quite good.¹⁷

We thank Professor J. I. Budnick, Professor G. Xiao, and Professor G. M. Luke for the use of their SQUID magnetometers. We also thank G. M. Ozeryansky, J. D. McCambridge, X. S. Ling, and R. J. Zieve for many helpful discussions. This work was supported by IGC-AS and the State of Connecticut, Department of Economic Development.

¹C. Meingast and D. C. Larbalestier, *J. Appl. Phys.* **66**, 5962 (1989); C. Meingast, P. J. Lee, and D. C. Larbalestier, *J. Appl. Phys.* **66**, 5971 (1989).

²P. J. Lee, J. C. McKinnell, and D. C. Larbalestier, *Adv. Cryo. Eng. (Mat.)* **36**, 287 (1990).

³G. L. Dorofeev, E. Y. Klimenko, S. V. Frolov, E. V. Nikolenkov, E. I. Plashkin, N. T. Salunin, and V. Y. Filkin, in *Proceedings 9th International Conference on Magnet Technology*, edited by C. Marinucci and P. Weymuth (Swiss Institute for Nuclear Research, Switzerland, 1985), p. 564.

⁴L. R. Motowidlo, B. A. Zeitlin, M. S. Walker, and P. Haldar, *Appl. Phys. Lett.* **61**, 991 (1991).

⁵K. Matsumoto, H. Takewaki, Y. Tanaka, O. Miura, K. Yamafuji, K. Funaki, M. Iwakuma, and T. Matsushita, *Appl. Phys. Lett.* **64**, 115 (1994).

⁶L. D. Cooley, P. J. Lee, and D. C. Larbalestier, *Appl. Phys. Lett.* **64**, 1298 (1994).

⁷R. W. Heussner, P. D. Jablonski, P. J. Lee, and D. C. Larbalestier, *IEEE Trans. Appl. Supercond.* **5**, 1705 (1995).

⁸M. K. Rudziak, J. M. Seuntjens, C. V. Renaud, T. Wong, and J. Wong, *IEEE Trans. Appl. Supercond.* **5**, 1709 (1995).

⁹P. Koorevaar, Y. Suzuki, R. Coehoorn, and J. Aarts, *Phys. Rev. B* **49**, 441 (1994).

¹⁰E. W. Collings, *A Sourcebook of Titanium Alloy Superconductivity* (Plenum, New York, 1983), Vol. 1, p. 420. $\xi_{\text{Nb}} \sim 15$ nm for cold-worked Nb that has $H_{c2} \sim 1$ T.

¹¹A hexagonal stack of 61 rods has 9 rods across the point to point diameter.

¹²L. D. Cooley and D. C. Larbalestier, in *Proceedings 8th U.S.-Japan Workshop on High-Field Superconducting Materials*, edited by K. Yamafuji and D. C. Larbalestier (Ministry of Education Science Technology, Gov. of Japan, U.S. Department of Energy, 1993), p. 92.

¹³Data for typical wires, IGC-Advanced Superconductors, 1875 Thomaston Ave., Waterbury, CT 06704.

¹⁴A Ti pin volume of 2.5% provided at most an additional 2 GN/m³. Cu is an even weaker pin than Ti. See Refs. 2 and 4.

¹⁵The elastic energy cost of vortices bunching up on the pins with spacing less than the equilibrium lattice spacing is much greater than the pinning energy gained with such bunching. We conclude that the vortices will have access to fewer pins as the field is increased. See, e.g., E. H. Brandt, *Phys. Rev. B* **34**, 6514 (1986).

¹⁶For conventional wires, one generally finds $F_p \propto b(1-b)$.

¹⁷We do not expect this form to hold for wires B and D, which also have interface pinning.